

# INVESTIGATION AND REPAIR OF HEAT EXCHANGER FLANGE LEAK

Dennis Martens

Michael A. Porter

## ABSTRACT

During original operations a leak developed in the bolted tube sheet joints of a stacked pair of type 321 stainless steel TEMA type BEU exchangers in  $8.27 \times 10^6 \text{ N/m}^2$  (1200psi)  $371 \text{ }^\circ\text{C}$  ( $700^\circ\text{F}$ ) Hydrogen and Oil service (see Figure 1). After unsuccessful attempts to repair the leak an evaluation of the flanged joint design was undertaken. Finite Element analysis of the tube sheet joint provided the basis for understanding the complex temperature profile, displacements and stresses in the joint. The exchanger was successfully repaired using a weld ring gasket closure with the addition of disc spring washers to the bolting (see Figure 2). Observation of the flanged joint during startup and operation confirmed the Finite Element Analysis results.

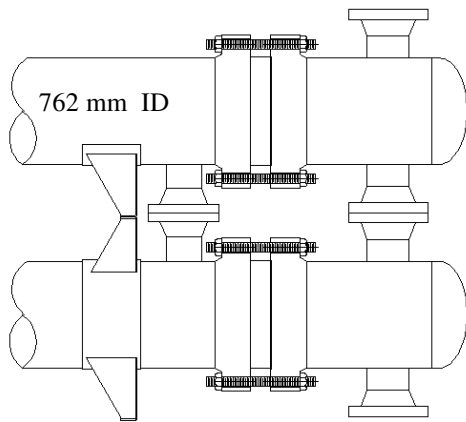


FIGURE 1 PARTIAL VIEW OF HEAT EXCHANGERS

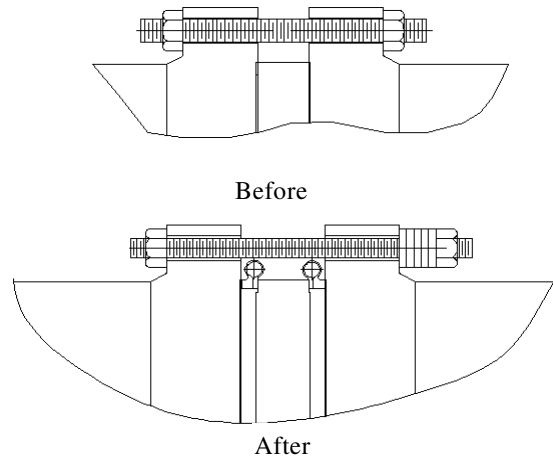


FIGURE 2 - BEFORE AND AFTER DETAIL OF JOINT

## DESCRIPTION OF PROBLEM

The exchangers developed leaks at the tube sheet gaskets during initial operation. A leak of hot oil and hydrogen from the tube sheet joint would result in fire potential, therefore it was decided to regasket the exchangers. It was noted that the exchangers had been successfully shop hydrotested and retested prior to initial operations. The stainless steel (B-8) bolting was found to be loose and it was assumed that inadequate bolt torque was the cause for the leakage. The exchangers were disassembled, inspected, regasketed, reassembled and bolting hydraulically torqued. The exchangers were subjected to a design pressure water leak test and proved leak tight. The unit was restarted and the exchangers operated for several days before the unit was shut down due to an instrument malfunction. The exchangers leaked on cool-down and retorquing of the bolting revealed that again the bolting had become extremely loose. On disassembly it was noted that one of the internal gage ring spiral wound gaskets had deformed in a manner similar to the first failed gasket as the outer

wraps had separated. The exchanger was regasketed again with even greater care and the bolting was hydraulically tensioned to design bolt stress instead of torqueing. The exchangers were again subjected to a design pressure water leak test, proved leak tight and the unit was restarted.

During the second disassembly, the design of the flanges was reviewed per ASME Section VIII Division 1 Appendix 1. The flange design was found to be in accordance with the code criteria. The solid 321 stainless steel flanges and B-8 bolting calculated rotation and stresses were considered to meet all design criteria.

The exchangers again leaked after a few days of operation and were hot torqued to stop the leaks. The exchangers were subjected to several minor process upsets during the next week of initial operations and again the gaskets leaked and the gaskets were replaced a third time. In many respects, this problem is very similar to that described by Winter (1989).

The design of the tube sheet joint was reviewed further with field measured operating temperature profile data and it became apparent that the bolting was being subjected to stresses in excess of yield during normal operation of the exchangers. This condition is not uncommon in bolted joints, however the joints were leaking even after the hot retorquing. Further investigation and calculations indicated that the bolting would yield enough during heat-up that on cool-down the bolt stress would not be sufficient to provide adequate gasket seating stress. It was decided to install disc spring washers to eliminate the bolt yielding condition and consideration was given to changing the bolting to B-7 materials, based upon the simplified calculation format below.

Estimated average bolt temperature 93 °C (200 °F)  
 Estimated average flange and tube sheet temperature  
 (for axial growth) 177 °C (350°F)

Delta Temp = 84 °C (150°F)

Coefficient of expansion ( $\alpha$ ) =  $1.62 \times 10^{-5}$  m/m °C  
 ( $9 \times 10^{-6}$  in/in°F)

Bolt modulus of elasticity @ 93 °C (200°F) (E) =  
 $1.79 \times 10^{11}$  N/m<sup>2</sup> ( $26 \times 10^6$  psi)

Bolt expected actual yield stress @ 93 °C (200°F) (Sy) =  
 $2.07 \times 10^8$  N/m<sup>2</sup> (30,000 psi)

Design bolt stress at assembly  $S_{ba} = 8.27 \times 10^7$  N/m<sup>2</sup>  
 (12,000 psi)

Additional bolt stress due to differential thermal expansion of  
 bolt and flange assembly ( $S_{be}$ ) =  $dT \alpha E$

Operating bolt stress  $S_{bo} = S_{ba} + S_{be}$

$S_{bo} = 8.27 \times 10^7 + 2.42 \times 10^8$   
 $= 3.25 \times 10^8$  N/m<sup>2</sup> (47,100psi)

This indicated stress exceeds the yield stress of the bolt material; therefore, the bolts have permanently stretched and the flange assembly has been subjected to 2.5 times design bolt force.

The stress reduction due to differential thermal shrinkage of the bolt and flange assembly during cool down ( $S_{bc}$ ) is equal to the increase in stress during heating ( $S_{be}$ ).

The cool-down residual bolt stress  $S_{br} = S_{bo} - S_{bc}$

$S_{br} = 2.07 \times 10^8$  (yield stress) -  $2.42 \times 10^8 = -3.4 \times 10^7$  N/m<sup>2</sup>  
 (-4900 psi)

Thus, the bolt would become totally unloaded when returning to ambient conditions.

During this design review it became apparent that there was a second condition that was contributing to the gasket leakage. The differential temperature profile indicated that the tube sheet was considerably warmer than the flanges and this was causing a differential radial expansion of the gaskets' surfaces relative to each other. The exchanger was a multi-pass on the tube side and this further complicated the differential expansion issue. The differential movement was quantified to be on the order of 0.9 to 1.0 mm (0.035 to 0.040") and was subjecting the gasket to a "scuffing" condition.

Estimated average tube sheet temperature = 316 °C (600°F)  
 Estimated average flange temperature = 177 °C (350°F)  
 Delta Temp. (dT) = 139 °C (250°F)  
 Approximate radius of gasket (r) = 0.406 m (16")  
 Coefficient of expansion ( $\alpha$ ) =  $1.62 \times 10^{-5}$  m/m °C  
 ( $9 \times 10^{-6}$  in/in°F)

Scuffing movement =  $r \alpha dT = 0.91$  mm (0.036")

This scuffing condition was discussed with gasket vendors. Although no criteria was available for the limits of scuffing, the movement was considered as possibly excessive for spiral wound gasket applications. This scuffing condition was considered to have damaged the gaskets enough that they were leaking in service even though the bolts had been hot torqued. The combination of bolt yielding due to differential temperatures and gasket scuffing was considered to be the cause for joint leakage.

Meanwhile the exchangers, after three attempts to stop the leakage had begun to leak with even the slightest variance in unit operating conditions. It was apparent that the problem had to be rectified quickly.

The hand calculations made earlier while not sufficient to fully define the joint movements and stresses, had qualified the reasons for the leaking joint. It was decided that the investigation of the temperature profiles, differential expansions and joint stresses would have to be undertaken by the use of Finite Element Analysis (FEA).

## FINITE ELEMENT SOLUTION

The FEA solution was conducted by Dynamic Analysis. The model for the analysis was based on the exchanger fabrication drawings and actual field temperature measurements. The exchanger tube sheet joint was also affected by the nozzle loads that it must withstand. Time constraints did not allow FEA development of interconnecting nozzle loads. Therefore, these were qualified by the use of piping stress analysis software. It was anticipated that these nozzle loads would not be the limiting or most disrupting factor for the joint and therefore it would be satisfactory to use less accurate values than a comprehensive FEA study would have produced.

The modeling of the temperature distribution required individual tube-pass calculated fluid temperatures in addition to the field operating temperature data. The tube sheet was anticipated to have considerable temperature-induced differential expansion relative to the shell and bonnet mating flanges and within itself. Therefore a three dimensional thermal model was determined to be the correct approach to simulate the field measured temperature profile. The data from the thermal study was then used for the stress analysis study.

### FEA MODEL SELECTION

Designing the FEA model for the analysis of this problem required several compromises. Most of the models used in the literature for examination of flange type geometries are constructed with axisymmetric elements. The primary advantage of axisymmetric elements is that they drastically reduce the problem size when compared to the use of three dimensional elements. While this flange system was, for the most part geometrically axisymmetric, the loading was not. The applied temperatures from the internal fluids was symmetric about the vertical plane of the vessel rather than axisymmetric. Additionally, there was a significant bending moment exerted on the flange by the attached piping forces. Thus it was necessary to use three dimensional elements in the modeling process.

Despite the necessity of using three dimensional elements, time was of the essence in the completion of the analysis. All of the modeling and analysis was completed using the PC based Algor, Inc. finite element software during the period from December 17 to December 31, 1992. That such a project could be undertaken and completed in such a short time period is a tribute to the state of the art in tools available to the engineering community today.

### MODEL DESCRIPTIONS

Three basic models were used in the analysis of this problem.

A thermal model comprised of approximately 6880 three dimensional solid brick elements was used to compute the temperature distribution in the flange system. Figure 3 illustrates the geometry of the thermal model. As may be seen, the symmetry about the vertical axis was used to cut the number of elements that might have been required by a factor of two. The vessel shells were modeled to a distance of approximately one diameter from the flange and terminated with boundary conditions. Although a shorter length of the shell would have been indicated by Saint Venant's principle, the longer length was

selected to account for the bending forces caused by the piping loads.

A linear stress model was constructed using the same geometry as the thermal model except that the bolts were modeled with beam elements rather than the brick elements used in the thermal model. This change facilitated the imposition of preloading on the flange system as well as reducing the problem size for the stress and deflection computations.

After the problem was defined and a potential solution was developed using the models above, an axisymmetric model was developed to examine the details of the proposed solution. Since the variations in the bolts loading around the flange had been determined from the three dimensional model, it was possible to determine the limiting cases and apply these to the axisymmetric model.

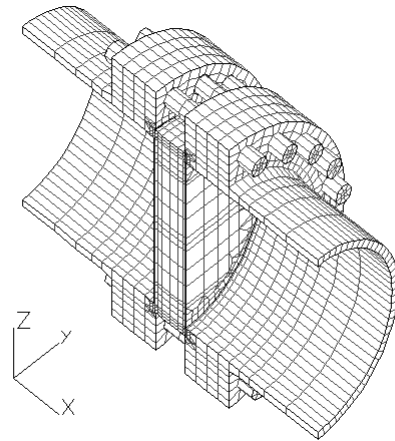


FIGURE 3 -THERMAL MODEL

### THERMAL RESULTS

The inlet and outlet fluid temperatures as well as the surface temperatures at several locations on the joint were obtained from the operating personnel. The conductive film coefficients on the model were adjusted so that the surface temperatures matched the field data with the applied internal temperatures. The resulting temperature distribution in the joint system is illustrated in Figure 4. As may be seen, there was a significant temperature gradient indicated in both the tube sheet and the flanges.

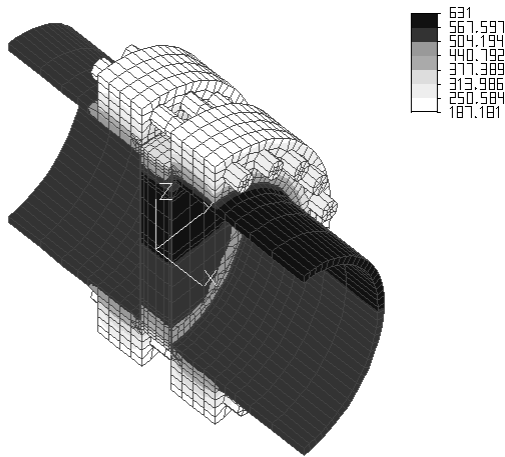


FIGURE 4 TEMPERATURE DISTRIBUTION IN FLANGED CONNECTION (°F)

Figures 5 and 6 illustrate the temperature profiles in the tube sheet and flanges respectively. It is instructive to note that while the range of temperatures in the tube sheet is nearly the same as in the flanges, the relative distribution is quite different. Most of the tube sheet is at a relatively high temperature while only a small outer ring is at a lower temperature. In the flanges, almost the opposite is true. Most of the flange is at a relatively low temperature, while a small portion at the interior of the flange is at an elevated temperature. These temperature distributions are responsible for the differences in the thermally induced radial growth between the tube sheet and flange that will be discussed in the next section.

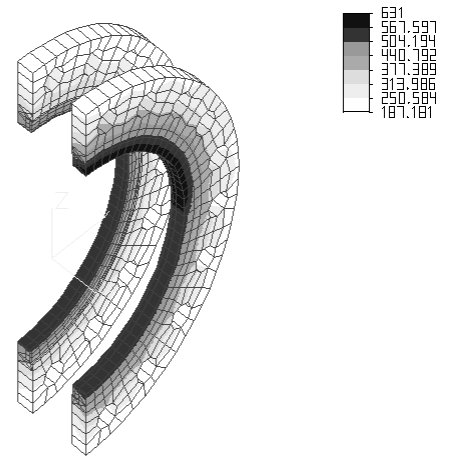


FIGURE 6 - TEMPERATURE DISTRIBUTION IN FLANGES (°F)

### THREE DIMENSIONAL STRESS MODEL AS BUILT

To compute the deflections and stresses in the joint system, the temperatures computed with the thermal model were transferred to stress model as previously described. In addition to the loads due to the temperature distributions, the internal pressure and the loading due to the piping forces and the preloading of the bolts had to be applied. In order to separate the deflections and stresses due to the primary (pressure and pipe force) loads from the secondary (thermal) loads, a series of load cases with various combinations of the above loads were developed. The load case combinations employed are illustrated in Table 1.

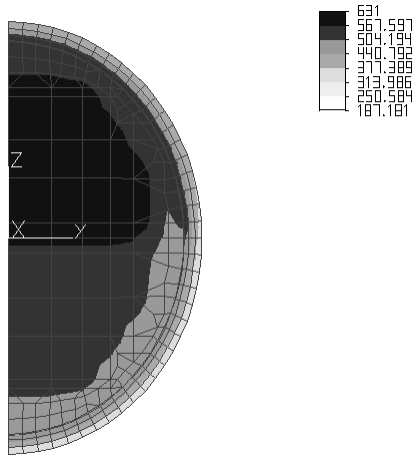


FIGURE 5 TEMPERATURE DISTRIBUTION IN TUBE SHEET (°F)

TABLE 1 - STRESS MODEL LOAD CASES

Load Case Number	Loads Applied
1	Bolt Preload Only (Hydro basis)
2	Bolt Preload + Thermal
3	Bolt Preload + Pressure
4	Bolt Preload + Pipe Forces
5	Bolt Preload + Pressure + Pipe Forces
6	All Loads

### THREE DIMENSIONAL STRESS MODEL RESULTS

#### Scuffing

Figure 7 illustrates the deflections in the model in the vertical direction. As may be seen, the deflection (expansion) of the tube sheet is greater than that of the flange. This differential deflection causes a scuffing of the gasket between the flange and the tube sheet. Due to the complexity of the temperature distribution in the tube sheet and, to a lesser extent, the flanges, the magnitude of

the radial scuffing is not a constant around the circumference of the vessel.

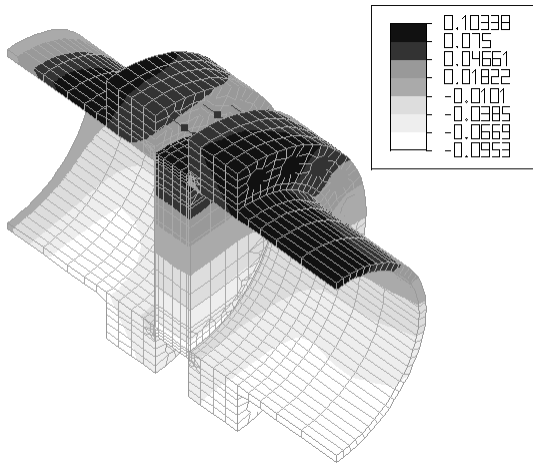


FIGURE 7 - VERTICAL DEFLECTIONS IN JOINT (INCHES)

Figure 8 illustrates the magnitude of this scuffing at selected locations on the gaskets between the tube sheet and the two flanges. As may be seen, the scuffing value varies by approximately 30% between the locations selected. Since the selected locations are simply at 45 degree intervals around the circumference, it is possible that the actual variation is even higher. The scuffing and/or the differential scuffing of the gasket is clearly a problem for this joint. This result confirms the preliminary qualifying calculations.

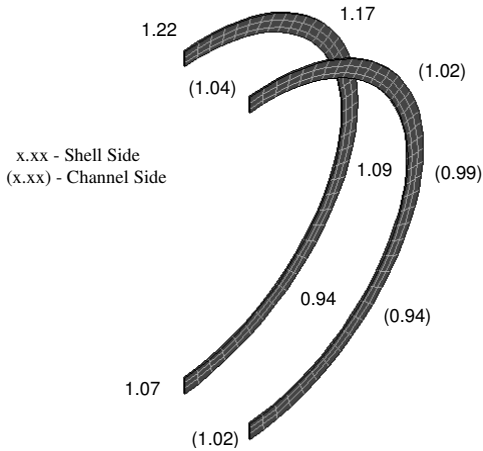


FIGURE 8 - GASKET SCUFFING (mm)

**Bolt loads**

Since the bolts in the field unit had become loose and required retorquing after start-up, the force and stress in the bolts during operation was of significant interest. Although all of the bolts were carefully torqued to the same value before start-up, it seemed likely that there would be a difference in the loads on the individual bolts due to the loading conditions. Figure 9 illustrates

the locations of the bolts on the flange model and a numbering system used to identify specific bolts.

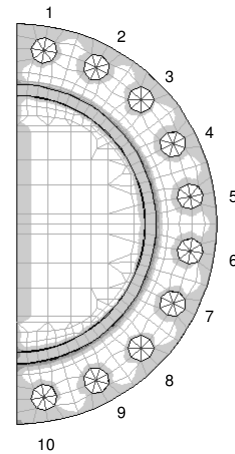


FIGURE 9 - BOLT LOCATIONS AND NUMBERING

TABLE 2 BOLT STRESSES AND FORCES - AS BUILT

Location Number	Bolt Stress - kN/m <sup>2</sup>					
	Load Case Number					
	1	2	3	4	5	6
1	128000	511000	125000	165000	162000	545000
2	128000	510000	125000	161000	158000	540000
3	128000	508000	124000	154000	150000	530000
4	128000	503000	124000	145000	141000	516000
5	128000	495000	124000	134000	130000	497000
6	128000	483000	124000	122000	119000	474000
7	128000	475000	124000	111000	108000	455000
8	128000	471000	124000	102000	101000	442000
9	128000	472000	125000	95000	91000	435000
10	128000	473000	125000	91000	88000	432000

Location Number	Bolt Load - N					
	1	2	3	4	5	6
1	5.07E+05	2.02E+06	4.93E+05	6.54E+05	6.40E+05	2.16E+06
2	5.07E+05	2.02E+06	4.93E+05	6.38E+05	6.24E+05	2.14E+06
3	5.07E+05	2.01E+06	4.92E+05	6.09E+05	5.95E+05	2.10E+06
4	5.07E+05	1.99E+06	4.91E+05	5.72E+05	5.57E+05	2.04E+06
5	5.07E+05	1.96E+06	4.91E+05	5.29E+05	5.14E+05	1.97E+06
6	5.07E+05	1.91E+06	4.91E+05	4.85E+05	4.69E+05	1.87E+06
7	5.07E+05	1.88E+06	4.91E+05	4.41E+05	4.26E+05	1.80E+06
8	5.07E+05	1.87E+06	4.92E+05	4.04E+05	3.99E+05	1.75E+06
9	5.07E+05	1.87E+06	4.93E+05	3.76E+05	3.62E+05	1.72E+06
10	5.07E+05	1.87E+06	4.93E+05	3.61E+05	3.47E+05	1.71E+06

Table 2 illustrates the stress in, as well as, the indicated force in each of the bolts for the 6 load cases examined. The initial preload condition indicates that the load in the bolts was uniform with a stress level near the allowable for the B8M bolts. In Load Case 2, where the temperature load is applied, the indicated stress in the bolts is well over the yield for this material. Thus, the bolts would be expected to stretch or elongate during this condition. When all loads are applied, the maximum indicated stress in the bolts is over  $5.45 \times 10^8 \text{ N/m}^2$  (79,000 psi). Additionally, the variation in the load from bolt to bolt is approximately 26%. At this point, we might expect some problems with the seal on the gasket due to the uneven loading and the scuffing mentioned in the previous section.

If we assume that the bolts will yield until the stress is lowered to the yield level of  $2.07 \times 10^8 \text{ N/m}^2$  (30,000 psi), we can compute the elongation or stretch of each of the bolts. For the above loading conditions, this results in elongation values ranging from 0.6 to 0.9 mm (0.023" to 0.035"). If the unit were then brought back to the unheated condition, this elongation would be sufficient to completely unload the bolts, consistent with the observed field conditions and qualifying calculations.

In fact, the conditions indicated in Table 2 do not indicate the severity of the actual conditions. Due to the complexity of the model and the time constraints imposed on the analysis only a steady state heat transfer analysis was conducted for this problem. As Sawa et al (1993) have demonstrated, however, the stress in the bolts due to the transient temperature conditions may be considerably higher than indicated by the steady state conditions. Using a relatively simple model (see Appendix for the development of the model) we can compute the relaxation in the bolt stress due to elongation during a temperature transient.

Assuming that the bolts reach their final temperature some time after the flanges, we can define a temperature lag as the difference between the final temperature of the bolts and the temperature of the bolts at the time the tube sheet and flanges reach their steady temperatures. Table 3 illustrates the stress in the bolts that would be developed as a function of this temperature lag. The difference between the indicated stress and the stress that would result from a 0 degree temperature lag is the unloading that would be expected after the bolts arrived at their steady state condition. As may be seen, this relaxation becomes very significant as the temperature lag increases.

TABLE 3 - BOLT RELAXATION DUE TO STRETCH CAUSED BY TEMPERATURE LAG

Temperature Lag °C	Bolt Stress - psi		Stress Unloading - psi	
	N/m <sup>2</sup>	psi	N/m <sup>2</sup>	psi
0	5.10E+08	74,100*		
-5	5.26E+08	76,200	1.50E+07	2,100
-10	5.41E+08	78,400	2.00E+07	4,300
-15	5.56E+08	80,600	4.50E+07	6,500
-20	5.71E+08	82,800	6.00E+07	8,700
-25	5.86E+08	84,900	7.50E+07	10,900
-30	6.01E+08	87,100	8.99E+07	13,000
-35	6.16E+08	89,300	1.05E+08	15,200
-40	6.31E+08	91,500	1.20E+08	17,400
-45	6.46E+08	93,600	1.35E+08	19,600
-50	6.61E+08	95,800	1.49E+08	21,700

(Note that the actual stress could not exceed the yield.)

\* This is the initial operating stress, which would exceed the yield of the bolts.

The stress in the bolts cannot, in general, exceed the material yield. Therefore, because of the combination of the differential loading due to pipe loads indicated in Table 2 and the potential relaxation due to temperature lag shown in Table 3, the potential for some of the bolts to become unloaded clearly exists. Between the scuffing of the gasket and the unloading of the bolts, the seal of this joint was at best tenuous. Note that the maximum temperature differential used in the above analysis is 50 °C, while the work by Nau and Watson (1985) indicates that the temperature lag could be substantially greater.

### Gasket Loading

The compressive stress in the gasket is an indicator of the ability of the joint to maintain a seal. In the model used for this analysis, however, the gasket was not modeled with nonlinear elements as would be required to accurately replicate the compression-only reaction of the gasket. Nonetheless, an examination of the stresses in the gaskets is useful from a qualitative standpoint.

Figures 10 and 11 illustrate the computed stresses in the gaskets as a function of the radial dimension of the gasket starting from the I.D. at 45 degree increments around the model starting at the top of the model. Figure 10 illustrates the stresses in the channel side gasket while Figure 11 illustrates the same in the shell side gasket. Note that the inner portion of the gasket (0-0.375 mm) is a solid stainless steel gage ring, while the remainder is the spiral-wound portion of the gasket. Also, it is important to remember that because this was a linear analysis, the actual stress levels would be considerable lower due to yielding in the material.

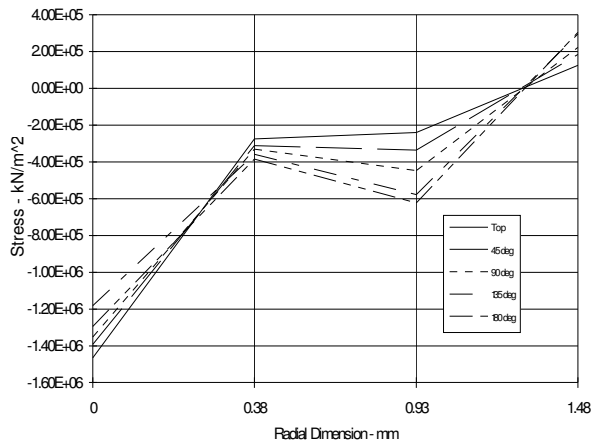


FIGURE 10 - GASKET STRESS - CHANNEL SIDE

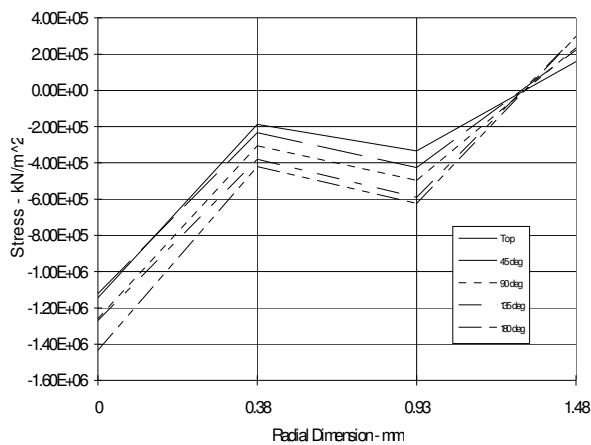


FIGURE 11 GASKET STRESS - SHELL SIDE

The fact that the outer edge of each gasket is indicated to be in tension (a physical improbability at best) makes the absolute values questionable. We may, however, see that there is a general trend toward unloading of the gasket at the top of the flange, especially in the shell side, due primarily to the piping loads. Additionally, the stresses shown here are a result of a linear analysis wherein the bolts have not been allowed to yield. Thus, if we allow for yield in the bolts, the potential for unloading of the gaskets is indicated.

### Flange Stresses

The indicated stress levels in the flanges due to the loading conditions imposed were well within the allowable levels for both the primary and secondary loads. The actual stresses due to the secondary loads would have been even lower than indicated due to the yielding that would have occurred in the bolts. One possible solution to this problem would be to replace the stainless steel B8M bolts with a higher yield carbon steel B7M bolt. When this was done in the model, the indicated stress in the flanges

became excessive. This increased stress was due to the lower coefficient of thermal expansion in the B7M material. A direct substitution of the bolt materials would likely have resulted in yielding in the flanges; subsequent leaks during thermal cycles would have been almost inevitable. In order to prevent flange deformation, the bolt forces should be limited to approximately  $8.9 \times 10^5$  N (200,000 pounds) per bolt.

### SUMMARY OF THREE DIMENSIONAL MODEL RESULTS

The three dimensional model indicated that the leaks in the joint were likely caused by a combination of two factors:

- The differential radial growth between the tube sheet and flanges (scuffing)
- The elongation of the bolts during system startup and operation

Replacing the stainless steel bolts with carbon steel bolts would likely result in warping of the flanges. Thus, the solution would have to involve more than a simple change of bolt material.

### SOLUTION EVALUATION

The solution proposed for this problem consisted of two basic changes to the flange joint.

- To control the scuffing problem, a "weld ring" gasket would be used in place of the original spiral-wound gasket.
- Carbon steel bolts with disk spring washers to control the maximum bolt load would be used in place of the stainless steel bolts.

In order to check the feasibility of these solutions, an axisymmetric model was developed. The axisymmetric model did not permit the evaluation of the load variation around the joint due to non-axisymmetric loading. It did, however, allow assessment of the radial displacement (scuffing) and the bolt loading due to the temperature distribution. To evaluate the variation in bolt loading, a separate run of the three dimensional model was conducted using the procedures for modeling the bolts which will be described in this section. The data from this three dimensional model provided bounds for the axisymmetric model.

Figure 12 illustrates the geometry of the axisymmetric model. The enlarged view provides more detail of the weld ring gasket geometry. Note that this type of gasket is machined in two separate pieces, mating in the center of the circular portion. The separate halves are welded to the flange and tube sheet faces and then welded together to form a sealed gasket. The interface between the two faces of the gasket was modeled both with non-linear gap elements and with connecting beam elements, as will be discussed in a later section. The bolts in the actual flange are periodic about the axis of symmetry rather than axisymmetric. Therefore, an equivalent beam element was used to model the bolts.

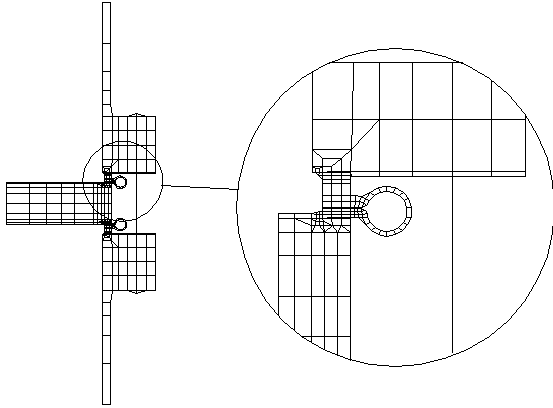


FIGURE 12 - AXISYMMETRIC MODEL

**Scuffing**

Figure 13 illustrates the radial (scuffing) motion of the two gasket faces for the shell side gasket. The shell side gasket in the axisymmetric model followed the three dimensional model in indicating the highest scuff values. As may be seen, a relative displacement of approximately 1.25 mm (0.05") was indicated between the two surfaces. This displacement was predicated upon the absence of radial force transfer between the surfaces.

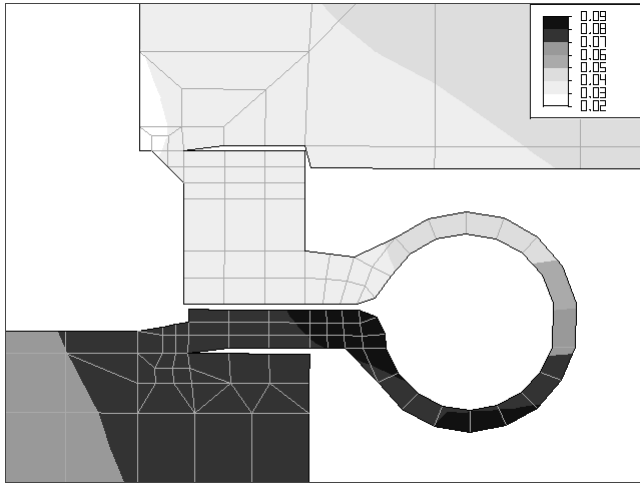


FIGURE 13 - RADIAL DISPLACEMENT (INCHES)

Although the gasket faces were to be lubricated, there was some concern about the tensile stress in the weld between the gasket and the tube sheet/flange. To assess this potential problem, the gasket faces were connected with beam elements. The properties of these elements were varied to simulate a radial force transfer between the two surfaces equivalent to the frictional force. Based upon these studies, the weld radius between the gasket and the adjoining parts was increased to the maximum that the existing geometry would allow.

Figure 14 illustrates the friction stress in the shell side gasket based upon a coefficient of friction of 0.4. As may be observed,

there is still an area of elevated stress near the gasket to flange weld. Since the load is a secondary load, however, the  $2.4 \times 10^8$  N/m<sup>2</sup> (35,000 psi) indicated should not pose a problem. When the coefficient of friction is raised to 0.8, the stresses in this area are nearly doubled. If the frictional force were actually this high, there would be concern for the weld between the gasket and tube sheet. We have concluded that the 0.4 value is probably a best guess for this geometry.

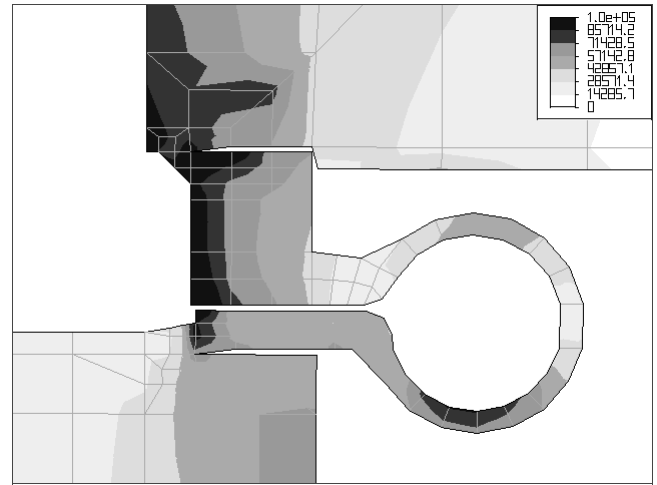


FIGURE 14 - RADIAL STRESS (PSI)

**Bolt Loading With Disk Spring Washers**

The evaluation of bolt loading with the disk spring washers was conducted with the three dimensional model by adjusting the properties of the bolts so as to simulate the stiffness of the washers.

TABLE 4 - BOLT FORCE WITH DISK SPRING WASHERS

Bolt Number	BOLT FORCE - N					
	LOAD CASE NUMBER					
	1	2	3	4	5	6
1	378,176	812,832	374,083	427,016	422,924	857,580
2	378,176	812,886	374,083	421,832	417,739	850,759
3	378,176	806,829	373,810	412,555	408,189	837,116
4	378,176	800,281	373,537	400,004	395,638	818,016
5	378,176	789,639	373,537	385,543	381,177	792,641
6	378,176	776,269	373,537	370,536	366,170	764,264
7	378,176	766,174	373,537	356,074	351,709	739,707
8	378,176	760,990	373,810	343,523	339,430	722,244
9	378,176	759,353	374,083	334,246	330,153	711,330
10	378,176	759,353	374,083	334,246	325,242	706,419

Table 4 illustrates the computed loads in the carbon steel bolts with the disk spring washers installed. (Note that the preload did not include the hydro load for this analysis.) As may be seen the computed loads are all below the allowable  $8.9 \times 10^5$  N (200,000 pound) load limit required to prevent flange deformation.



**FIELD INSTALLATION AND RESULTS**

The disc spring washers were specified from the FEA data to accommodate a bolt-up loading of  $3.6 \times 10^5$  N (80,000 lb) force and 1.8 mm (0.070") delta compression for operating, providing  $8 \times 10^5$  N (180,000 lb) bolt force in operation. This resulted in a four disc washer stack arranged in a two cup configuration which would accommodate 150% of design compression. The disc spring washers were purchased from a well known supplier.

The B-8 bolting was replaced with B-7 material of a slightly smaller diameter. The use of the disc spring washers eliminated the concern for dissimilar flange and bolting thermal expansion coefficients by replacing the bolting material elasticity modulus with the spring rate of the washers.

The weld ring gaskets were not available from the normal suppliers in the time frame selected for shut down and repair. Therefore detailed shop drawings were prepared from the gasket FEA study based on 1.24 mm (0.045") design radial differential growth of the tube sheet and mating flanges. The weld ring gasket half sections were machined from plate materials to maintain schedule requirements. The gaskets were match marked for assembly and grooves were ground in the interior contact lands to facilitate draining of process fluid from the gasket.

Prior to shut-down of the exchangers the position of the tube sheet outside diameter was observed to be nearly in contact with the outside diameter of the gasket surface relief in the shell flange. After cool-down the tube sheet position was confirmed to have moved approximately 0.89 mm (0.035") radially from its hot position relative to the shell flange gasket surface relief which was in agreement with the FEA results. The exchangers were disassembled after normal shut-down and pre-maintenance procedures were completed. It was noted that two of the four gaskets had damage to the outside spirals and one of the damaged gaskets had two outside metallic spirals extruded from the gasket retaining groove.

The weld ring gasket half sections were indexed to maintain match marks, clamped to the flange faces and the fillet attachment welds were made. The exchangers were assembled, including the bonnets, and a few bolts installed to aid alignment. The closing weld on the outside of the gasket was then completed, the bolts hydraulically torqued and the compression of the disc spring washers monitored. The compression of the washers and the hydraulic torque progress tracked well and the final washer compression was in good agreement to the calculated amount based on design bolt torque. The exchangers were subjected to a design pressure hydrotest to prove leak tightness. The complete repair procedure required six days from disassembly through hydrotesting.

The unit was then started up and as the normal exchanger temperature was established the compression of the disc spring washers was observed. The field measured compression was in good agreement with the FEA-calculated movements. Table 5 below lists the data for a particular bolt and associated disc spring washer; both calculated and field observed data are presented.

**TABLE 5 - WASHER COMPRESSION AND BOLT LOADS**

Condition	Washer Compression Calculated	Washer Compression Measured
-----------	-------------------------------	-----------------------------

Bolt Up Compression	1.32 mm (0.052") <sup>1</sup>	1.73 mm (0.068")
Bolt load	$3.34 \times 10^5$ N (75,000 lb)	$4.32 \times 10^5$ N (97,000lb) <sup>1,2</sup>
Operating Compression	2.87 mm (0.113") <sup>1</sup>	2.59 mm (0.102")
Bolt load	$7.21 \times 10^5$ N (162,000 lb)	$6.49 \times 10^5$ N (146,000lb) <sup>1</sup>

<sup>1</sup> This washer compression or bolt load is based on spring rate tables for the disc spring washers

<sup>2</sup> Hydraulic torque was set to obtain  $4.0 \times 10^5$  N ( 90,000 lb) bolt load

The operating temperature profile of the flanges, tube sheet and bolts was measured and was found to be in close agreement to the temperatures obtained earlier and used for the calculation basis.

**TABLE 6 -MEASURED TEMPERATURE PROFILE**

Shell flange OD	100 °C (212°F)
Channel Flange OD	116 °C (240°F)
Bolts	93 °C (200°F)
Tube sheet OD	169 °C (336°F)
Process fluid into tube sheet	332 °C (630°F)
Process fluid exit shell pass	321 °C (610°F)

**CONCLUSIONS**

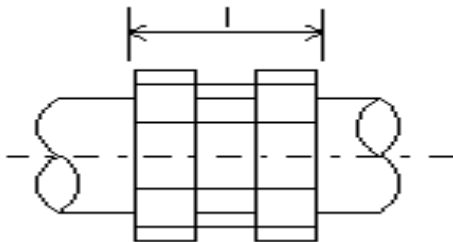
The exchanger leakage was caused by two conditions that effected the gaskets' ability to maintain a pressure seal. The two conditions were excessive bolt loading and gasket scuffing, both due to differential thermal expansion of the assembly. The standard flange design approach was used, however the effect of differential thermal expansions was not investigated during the design stage. Simple hand calculations would have been sufficient to qualify these problems and perhaps allow mitigation at the design stage, but to quantify the design values, a complete FEA study was required.

The first condition of excessive bolt loading variance due to differential temperatures within the flange, bolt and tube sheet assembly was predictable at the design stage. The current knowledge of temperature profiles of flanged joints is somewhat limited and our first FEA work did not produce as extreme a differential temperature between the bolts and flange/tubesheet as was field verified. It would have been difficult to establish a temperature profile during the design stage that would have duplicated the field data. The design could have assumed a differential temperature based on the bolt being exposed to an extreme ambient condition such as rain to establish a minimum bolt temperature near ambient temperature. This temperature when compared to the flange/tubesheet fluid temperatures would have resulted in a conservative bolt loading on the flange and gasket. This loading would have resulted in excessive gasket loading and flange rotation. The use of disc spring washers would have been recommended to replace the bolt modulus of elasticity with the disc washer spring rate which is approximately 10% of the bolt modulus of elasticity. The conclusion is that the effects of thermal expansion should have been examined in the design stage.

The second condition, gasket scuffing, could also have been predicted at the design stage if an adequate design temperature profile had been established. However, there is very little published information available on this type of gasket surface movement versus gasket sealing ability. It should be noted that the last gasket replacement and start up, prior to the installation of the weld ring gasket, was conducted with utmost care. During this time it is believed that the bolts reached their yield stress sometime during startup and were near yield stress during operation. Even with this extra care the gaskets started leaking shortly after startup. While it is not possible to state that the original gasket design would be expected to leak even with the use of disc spring washers, it is the authors' opinion that the gasket seal would not be adequate for the service. This is based on actual observed conditions and gasket manufacturer's concern that the calculated scuffing value was excessive for an internal gage ring spiral-wound gasket application. The manufacturers, however, did not have firm data to confirm their concern. The development of data relating to gasket scuffing would be necessary to provide a reliable basis to make a serviceability decision. This leads to the conclusion that in situations which require reliable gasket sealing, the assembly should be investigated for a gasket scuffing condition. The amount of the scuffing versus the ability of the gasket to reliably seal will become an engineering judgment decision until additional data and design rules are developed.

## RECOMMENDATIONS

1. The phenomenon of gasket scuffing should be studied to quantify the magnitude of potential problems.
2. More information concerning the actual temperature profiles in similar joints should be developed.
3. Solid models rather than simple axisymmetric models should be employed when using FE methods to predict gasket loads and stresses in similar joints where the loading is asymmetric.



# Appendix

## Bolt Thermal Expansion Stresses

- $\alpha$  Thermal Expansion Coefficient - in/in Deg F
- E Young's Modulus - lb/in<sup>2</sup>
- l Length - in
- dT Temperature rise above ambient - Deg. F

Tube Sheet Properties:  $E_b := 25.9 \cdot 10^6 \cdot \frac{\text{lb}}{\text{in}^2}$   
 $\alpha_b := 9.3 \cdot 10^{-6} \cdot \frac{\text{in}}{\text{in}}$   $dT_b := 120$   $l_b := 20 \cdot \text{in}$

Flange Properties:  $E_f := 25.9 \cdot 10^6 \cdot \frac{\text{lb}}{\text{in}^2}$   
 $\alpha_f := 9.3 \cdot 10^{-6} \cdot \frac{\text{in}}{\text{in}}$   $dT_f := 440$   $l_f := 14 \cdot \text{in}$

Bolt Properties:  $E_t := 25.9 \cdot 10^6 \cdot \frac{\text{lb}}{\text{in}^2}$   
 $\alpha_t := 9.3 \cdot 10^{-6} \cdot \frac{\text{in}}{\text{in}}$   $dT_t := 400$   $l_t := 6 \cdot \text{in}$

Thermal expansion of Flange and Tubesheet:

$$\delta_f := \alpha_f \cdot l_f \cdot dT_f + \alpha_t \cdot l_t \cdot dT_t$$

Thermal expansion of Bolt:

$$\delta_b := \alpha_b \cdot l_b \cdot dT_b$$

Stretching of Bolt:

$$\delta_{bs} := \delta_f - \delta_b \quad \delta_{bs} = 0.057 \cdot \text{in}$$

The stress in the bolt is:

$$\sigma_b := \frac{\delta_{bs} \cdot E_b}{l_b} \quad \sigma_b = 7.419 \cdot 10^4 \cdot \frac{\text{lb}}{\text{in}^2}$$

This can also be expressed in a more complete form as:

$$\sigma_b := E_b \cdot \left[ \frac{(\alpha_f \cdot dT_f \cdot l_f + \alpha_t \cdot dT_t \cdot l_t) - \alpha_b \cdot l_b \cdot dT_b}{l_b} \right]$$

$$\sigma_b = 7.419 \cdot 10^4 \cdot \frac{\text{lb}}{\text{in}^2}$$

## REFERENCES

- Andreosso, S., Flesch, B., and Bouche, D., "Parameters Governing Mechanical and Thermal Behavior of the Bolted Flange - Simplified Method," *The 1985 Pressure Vessels and Piping Conference*, Vol 98-2, pp. 129-135.
- Bickford, J.H., "Nuclear Bolting Issues and Programs," *The 1985 Pressure Vessels and Piping Conference*, Vol 98-2, 1985, pp. 105-109.

Blach, A.E., "Bolted Flanged Connections with Full Face Gaskets in Dissimilar Pairs," *The 1985 Pressure Vessels and Piping Conference*, Vol 98-2, 1985, pp. 137-144.

Chao, R.C., "Behavior of Bolted Flanges at Elevated Temperature-Program Overview," *The 1985 Pressure Vessels and Piping Conference*, Vol 98-2, 1985, pp. 117-123.

Hayashi, K. and Chang, A.T., "Section III - Development of a simple Finite Element Model of an Elevated temperature Bolted Flange Joint," *Welding Research Council Bulletin 341*, 1989, pp. 10-20

Nau, B.S. and Watson, S., "Computer Modeling of Thermal Lag Effects in Bolted Joints," *The 1985 Pressure Vessels and Piping Conference*, Vol 98-2, 1985, pp. 125-128.

Sawa, T, Hirose, T., and Kumano, H., "Behavior of Pipe Flange Connection in Transient Temperature Field," *ASME Journal of pressure Vessel Technology*, Vol. 115, Number 2, 1993, pp. 142-146

Wesstrom, D.B. and Bergh, S.E., "Effect of Internal Pressure on Stresses and Strains in Bolted-Flanged Connections," *ASME Transactions*, 1951, pp. 121-137.

Winter, J.R., "Section II - Historical Review of a Problem Heat Exchanger," *Welding Research Council Bulletin 341*, 1989, pp. 3-9

Winter, J.R. and Leon, G.F., "Radially Inward Buckling of Spiral Wound Gaskets," *The 1985 Pressure Vessels and Piping Conference*, Vol 98-2, pp. 111-116.